Spectral Distributions of "Trap" Pigments in the RC, CP47, and CP47−RC Complexes of Photosystem II at Low Temperature: A Fluorescence Line-Narrowing and Hole-Burning Study

F. T. H. den Hartog,[†] J. P. Dekker,[‡] R. van Grondelle,[‡] and S. Völker*[,†,‡]

Center for the Study of Excited States of Molecules, Huygens and Gorlaeus Laboratories, University of Leiden, P.O. Box 9504, 2300 RA Leiden, The Netherlands, and Department of Biophysics, Faculty of Physics and Astronomy, Free University, De Boelelaan 1081, 1081 HV Amsterdam, The Netherlands

Received: August 5, 1998; In Final Form: October 20, 1998

Broad-band absorption and fluorescence, fluorescence line-narrowing (FLN), and spectral hole-burning experiments have been performed on the Q_y-band of three subcore reaction-center complexes of photosystem II between 1.2 and 4.2 K: the isolated reaction center (RC), the inner core antenna CP47, and the CP47−RC complex. In the RC, fluorescence line-narrowing (FLN) is observed for excitation wavelengths $\lambda_{exc} \geq 676$ nm, whereas in CP47, this occurs for $\lambda_{exc} \geq 680$ nm. The FLN spectra of CP47−RC appear to be the sum of the individual spectra of the RC and CP47, an indication that this complex has two "traps". This has been confirmed from the spectral distributions obtained by measuring the hole depth (at constant hole width) as a function of λ_{exc}, as previously done for the RC [Groot, M. L., et al. *J. Phys. Chem. 100*, **1996**, 11488]. The maxima of these distributions are at ∼682 nm for the RC "trap" and at ∼690 nm for the CP47 "trap" within the CP47−RC complex. Further support that the two distributions of pigments in CP47−RC belong indeed to "trap" pigments is provided by the "effective" homogeneous line width Γ'_{hom} determined as a function of temperature for various excitation and detection wavelengths.

1. Introduction

The photosystem II (PS II) in green plants and algae is responsible for the splitting of water into oxygen, electrons, and protons in photosynthesis.[1] It is a large supramolecular pigment−protein complex embedded in the thylakoid membrane, which consists of a central core and a peripheral antenna, the latter known as light-harvesting complex II (LHC II).[2] LHC II collects energy of the sun and transfers it to the central core.[3] This central core contains the RC and the inner antenna complexes CP47 and CP43, in addition to a 33 kDa subunit and some minor proteins of low molecular mass.[2,4] In the RC, the excitation energy is converted into a charge separation, which eventually leads to a chemical potential used to split water and release oxygen.

The smallest unit in PS II that shows photochemical activity is the isolated reaction center (RC).[5] It contains six chlorophyll *a* (Chl *a*), two pheophytin *a* (Pheo *a*), and one or two β-carotene (β-Car) molecules,[1,6] which are bound to a complex formed by the D1 and D2 polypeptides, the cytochrome *b*559, and the psbI gene product; plastoquinone is lost during isolation. Recently, the structure of a complex of the RC with CP47 has been determined with 8 Å resolution.[7] It is generally accepted that the D1 and D2 proteins show large similarities with the L and M subunits of purple bacterial reaction centers.[8] On the basis of this fact, detailed models have been proposed for the RC structure of PS II.[9,10]

Much work has been reported on the spectroscopy of the RC,[3,11−13] but little is known about that of CP47. This protein, proximate to the RC, is the last one to be separated from the RC during isolation. CP47 probably comprises six hydrophobic transmembrane-spanning α-helices[14] that bind (14 ± 1) Chl *a* molecules[15,16] and two β-carotenes. Fluorescence and triplet-minus-singlet spectra of CP47 and CP47−RC at 4.2 K were reported to have broad bands at 690 ± 1 nm, which were attributed to pigments absorbing in the red-most wing of their inhomogeneous distributions.[6,16,17] Upon an increase of the temperature to 270 K, the fluorescence maximum shifts to ∼683 nm,[17] in accordance with a Boltzman distribution. In CP47, probably only one pigment gives rise to the emission band.[18]

One would expect that complexes such as CP47−RC trap a considerable fraction of the excitation in the lowest lying states of CP47 at sufficiently low temperatures.[17] However, it was concluded from spectral hole-burning experiments on CP47 at 4.2 K that the lowest state absorbing at ∼690 nm has a dephasing time of ∼50 ps[16] and could, therefore, not be attributed to "trap" pigments. The authors of ref 16 assumed that the state absorbing at ∼690 nm is excitonically correlated with another, higher lying, unobserved state at 687 nm that relaxes to it in about 70 fs. They further associated a 684 nm band in CP47 with "linker" Chl *a* molecules located in the exterior region of the RC complex[19] that relax down to the 687 nm state in 10 ps.[16]

To clear up these contradictions, one has to disentangle the spectral distributions of pigments hidden under the broad heterogeneous absorption bands. For this purpose, we have performed two types of experiments: fluorescence line-narrowing (FLN) at 1.2 K as a function of excitation wavelength λ_{exc} on the RC, CP47, and CP47−RC complexes and hole-burning (HB) on CP47 and CP47−RC as a function of λ_{exc}, detection wavelength λ_{det}, and temperature between 1.2 and 4.2 K. We compare the results of the three complexes with each

* To whom correspondence should be addressed.
[†] University of Leiden.
[‡] Free University.

10.1021/jp9832793 CCC: $15.00
Published on Web 12/09/1998

other and with those previously obtained for the RC by FLN[20] and by HB.[21] The main focus of this paper is the identification of "trap" pigments and their association with low-frequency modes. We show that the CP47 and CP47−RC complexes at low temperature have distributions of pigments absorbing in their red-most wing at ∼690 nm, which act as "traps" for the excitation energy and, therefore, do not transfer energy. Further results on CP47−RC suggest that its fluorescence originates from two types of "trap" pigments, the CP47 component at 690 nm and the RC component absorbing at ∼682 nm. The temperature dependence of the "effective" homogeneous line width Γ'_{hom} resulting from optical dephasing of both "trap" pigments resembles that of doped organic glasses. In a separate study, the time dependence of Γ'_{hom}, which gives information on the distribution of relaxation rates of the protein, is presented.[22]

2. Experimental Section

CP47−RC complexes were isolated from spinach, as described in refs 23 and 24 by incubation with the nonionic detergent *n*-dodecyl-β,D-maltoside (DM) and separation by ion-exchange chromatography. The isolated reaction center (RC), also called the D1-D2-cytochrome *b*559 complex, was obtained from CP47−RC by means of a short Triton X-100 treatment.[25,26] CP47 was separated from CP47−RC[27] and repurified to remove any free pigments.[17] The latter step was achieved by desalting the CP47 complexes on a PD10 column, subsequently loading them on a Q-Sepharose anion exchange column, and then eluting them with a buffer containing 35 mM $MgSO_4$. This procedure removed all chlorophylls disconnected from the protein.

Prior to the low-temperature measurements, the RC complexes were diluted in a buffer containing 20 mM bisTris (pH 6.5), 20 mM NaCl, 0.03% (w/v) DM, and 85% (v/v) glycerol. The CP47−RC and CP47 complexes were diluted in the same buffer at a glycerol concentration of ∼70% (v/v). All samples had an optical density OD ≈ 0.1 and were stored at 77 K when not used. To obtain glasses of good optical quality at liquid-helium temperature, the samples were slowly cooled (in about 10 min) from room temperature to 77 K by keeping the cuvette (thickness 3 mm) in an empty ^{4}He bath cryostat, of which the outer mantle was filled with liquid nitrogen. Cooling from 77 to 4.2 K was achieved in a few minutes by filling the cryostat with liquid helium. The temperature of the sample, varied between 4.2 and 1.2 K, was controlled by the vapor pressure of ^{4}He. It was measured with an accuracy better than 0.01 K using a calibrated carbon resistor in contact with the sample.[21]

Broad-band absorption and fluorescence excitation spectra were taken at 1.6 K with a tunable CW dye laser (Coherent 599-21, DCM dye, bandwidth ∼30 GHz = 1 cm^{-1} without intracavity assembly, amplitude stabilized to <0.5% by an electro-optic modulator) pumped by an Ar^+ laser (Coherent Innova 310). The laser was scanned with a linear actuator (Oriel, Encoder Mike 18246) controlled by a PC. Its wavelength was calibrated with a Michelson-type interferometer (home-built, accuracy ∼50 MHz). The excitation power density P/A (with P the power and A the area of the laser beam incident on the sample) was typically a few $\mu W/cm^2$. Transmission and fluorescence signals were detected with a cooled photomultiplier (PM, EMI 9658 R). The fluorescence signal was measured in a direction perpendicular to the exciting laser beam. To separate the fluorescence from scattered laser light, several long-wavelength-pass filters (Schott RG715, total thickness ∼1.5 cm) were put in front of the PM such that $\lambda_{det} \geq 715$ nm. Absorption spectra were obtained by dividing the transmission signal $I_t = I_0 \times 10^{-OD}$ at each wavelength by a reference spectrum $I_0(\lambda)$ of an empty cuvette and taking the logarithm of the ratio, $OD = \log(I_0/I)$, the absorbance or optical density.

Broad band fluorescence spectra were recorded by exciting the sample at 1.2 K at a fixed wavelength, $\lambda_{exc} < 676$ nm, with the laser at an excitation power density $P/A \approx 10$ mW/cm^2. The emission signal from the sample was detected through a scanning 0.85 m double monochromator (Spex 1402, resolution ∼5 cm^{-1}). Fluorescence line-narrowing spectra were taken with the same setup as the broad-band fluorescence spectra, but the samples were excited in the Q_y 0−0 band at $\lambda_{exc} \geq 676$ nm with a power density of 2−5 mW/cm^2 and the double monochromator was scanned at a higher resolution of ∼1 cm^{-1}. During the scan time of a spectrum, which was typically 5 min, the fluorescence signal decreased less than 8% due to hole burning.

Spectral hole-burning experiments were performed with the same CW dye laser but now in its single-frequency version (with an intracavity assembly, $\Gamma_{laser} \approx 2$ MHz). Burning power densities were in the range $P/A \approx 1$ $\mu W/cm^2$ to 1 mW/cm^2, and burning times varied from $t_b = 10$ s to $t_b = 200$ s. Thus, burning fluence densities varied between $Pt_b/A \approx 50$ $\mu J/cm^2$ and 70 mJ/cm^2. The holes were probed by means of fluorescence excitation (with $\lambda_{det} \geq 715$ nm) with the laser power attenuated by a factor 10^2-10^3.

In CP47−RC, holes were burnt at $\lambda_{exc} = 682$ nm and monitored as a function of detection wavelength λ_{det}. The fluorescence wavelength in these experiments was selected with the 0.85 m double monochromator with a spectral window of ∼0.6 nm. Such a window of ∼300 GHz is still much wider than the holewidths of a few gigahertz. The delay time between burning and probing the hole was fixed at $t_d \approx 200$ s.

The "effective" homogeneous line width Γ'_{hom} was determined from the hole width, measured as a function of burning fluence density Pt_b/A, extrapolated to $Pt_b/A \rightarrow 0$.[28,29] The holewidths were fitted with Lorentzian curves. Since, in these experiments, the burning time t_b, the delay time t_d, and the probe time t_p were within the same order of magnitude, the expression for Γ'_{hom} reduces to[29]

$$\Gamma'_{hom} = \frac{1}{2}\Gamma'_{hole,Pt/A\rightarrow 0}(t_d \approx t_b) - \Gamma_{laser} \qquad (1)$$

We neglected the bandwidth of the laser, $\Gamma_{laser} \approx 2$ MHz, because it was much smaller than the hole widths of a few hundred megahertz to a few gigahertz. Γ'_{hom} includes a contribution of spectral diffusion (SD)[22] corresponding to a delay time $t_d \approx 200$ s used in the present experiments.

3. Results and Discussion

3.1. Broad-Band and Line-Narrowing Spectra at Low Temperature. Figure 1a shows the absorption spectra of the three subcore complexes of PS II studied: the RC, CP47, and CP47−RC at 1.6 K. The areas of the RC and the CP47 spectra were taken proportional to the ratio of the number of chlorophyll-like pigments bound to them, i.e., 8:14. Their intensities were normalized in such way that the sum of the RC and CP47 spectra resembles the spectrum of CP47−RC. The result of this sum (dotted line) is a spectrum similar to that of CP47−RC but misses the double maximum at around 670−675 nm. This suggests that either one or two pigments of CP47−RC were lost on separating the RC from CP47, or that it is due to interaction between CP47 and the RC, or that the disorder of the pigments within the protein increased. The second derivatives of the individual absorption spectra are given in the lower

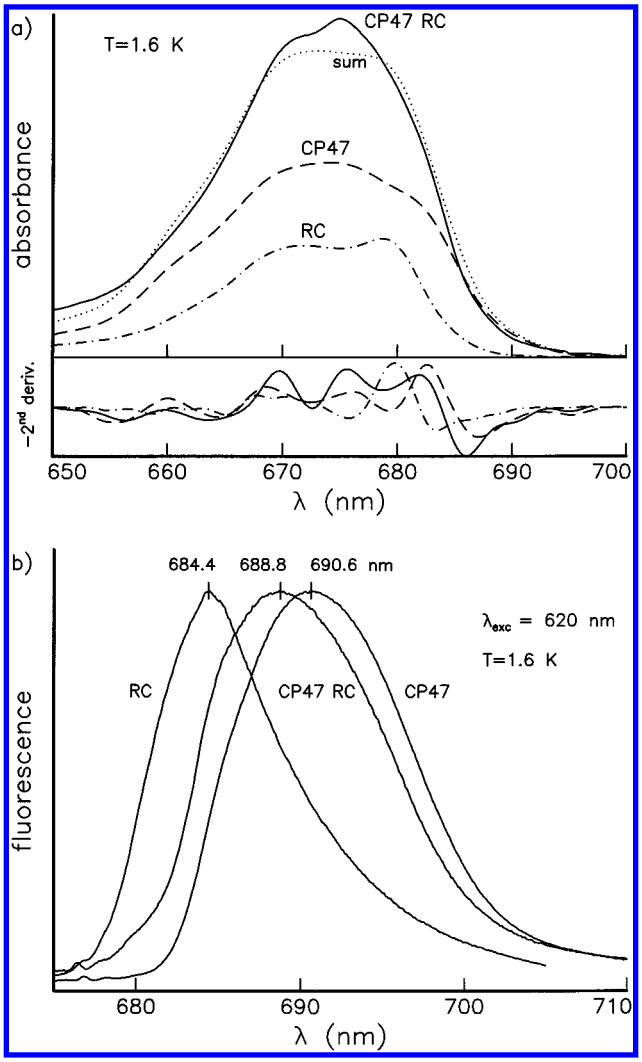

Figure 1. (a) Absorption spectra in the Q_y-region of the isolated reaction center RC, the core antenna CP47, and the CP47−RC complex of photosystem II at 1.6 K. The spectra of the RC and CP47 are normalized in such a way that the ratio of their areas is equal to the ratio of the number of pigments that are bound to these complexes, i.e., RC/CP47 = 8:14. The spectrum of CP47−RC has been normalized (its area) as closely as possible to the sum of the RC and CP47 spectra (dotted line). The lower part of the figure shows the second derivatives of the spectra. (b) Broad-band fluorescence spectra of the three complexes RC, CP47, and CP47−RC at 1.6 K excited at 620 nm with a laser power density of $P/A \approx 10$ mW/cm^2. The heights of the maxima of the spectra were normalized.

part of Figure 1a. The positions of the maxima are in good agreement with values previously reported for these complexes.[16,17,27,30] The optical densities of the samples were OD = 0.1−0.15.

Broad-band fluorescence spectra of the three subcore complexes at 1.6 K, excited at 620 nm, are depicted in Figure 1b. Their maxima were normalized. The position of the maximum and the shape of the RC spectrum are in good agreement with the values reported in refs 20 and 31. It has previously been shown by us that the emission in the RC is mainly due to a distribution of "trap" pigments absorbing around 682 nm that are not involved in energy transfer.[21,32] The fluorescence bands of CP47 and CP47−RC are red-shifted with respect to that of the RC, suggesting that excitation at 620 nm induces "downhill" energy transfer within their absorption bands to "trap" pigments of CP47 and CP47−RC absorbing at lower energies than the "trap" of the RC. If only the "trap" pigments of CP47 were responsible for the fluorescence spectra in the CP47 and CP47−RC complexes, one would expect the fluorescence bands of these two complexes to coincide, which is not the case. Figure 1b shows that the maximum of the CP47−RC emission is slightly (less than 2 nm) blue-shifted with respect to that of CP47. This difference may be due to either different Stokes shifts of the two complexes (i.e., variations in electron−phonon coupling strengths) or to a mixed fluorescence arising from the separate CP47 and RC components of CP47−RC. The experiments presented below prove that the latter is the correct explanation.

To characterize the spectral distributions of "traps" in these complexes, we have performed a series of fluorescence line-narrowing (FLN) experiments at 1.2 K, at different excitation wavelengths, see Figures 2 and 3. The results for the RC are shown in Figure 2a. Fluorescence spectra were recorded between 675 and 710 nm, with λ_{exc} varying stepwise from 620 to 692 nm. Two types of spectra can be distinguished, depending on whether λ_{exc} is smaller or larger than 676 nm. On excitation to the blue side of 676 nm, the spectra have nearly identical shapes: the emission is broad with a maximum at ∼684 nm and results from nonselective "downhill" energy transfer from higher lying pigments to the "traps"; see also Figure 3a in which the wavelengths of the emission maxima λ_{em} are plotted as a function of λ_{exc}.

On excitation of the RC to the red side of 676 nm, fluorescence line-narrowing (FLN) is observed because of the (direct) excitation of "traps". The vibronic structure that appears is best resolved whenever λ_{exc} is chosen close to the maximum of the absorption band of the "traps" at 682 nm.[20,21] We have previously proven by HB that there are "trap" pigments in the RC that absorb at this wavelength.[21] These "traps" show a small value of Γ'_{hom} (tens to hundreds of megahertz), which extrapolates to $\Gamma_0 = (2\pi\tau_{fl})^{-1}$ $T \rightarrow 0$, with $\tau_{fl} = 4 \pm 1$ ns being the fluorescence lifetime of the "traps". Our FLN results are in agreement with spectra previously reported, which were recorded over a wider frequency range of the emission at constant λ_{exc}.[20] Prominent in the spectra is a sharp peak at ∼20 cm^{-1} from the laser excitation wavelength, which shifts together with λ_{exc}; see also Figure 3a. This implies that no energy transfer occurs in this spectral region. The slope $d\lambda_{em}/d\lambda_{exc} = 1$ in Figure 3a further indicates that the homogeneous line width Γ'_{hom} is much smaller than the inhomogeneous line width, in accordance with ref 21. Low-frequency modes of ∼15−35 cm^{-1} in photosynthetic pigment−protein complexes have been attributed in ref 33 to protein modes. The same type of modes are characteristic for organic glassy materials.[34,35] In the RC, the ∼20 cm^{-1} mode has previously been observed by hole burning[19,36] as well as by FLN experiments.[20] In the experiments of ref 20, further low-frequency modes were identified at 37 and 80 cm^{-1}. In our spectra, a mode at ∼40 cm^{-1}, though poorly resolved, can be discerned. The 80 ± 5 cm^{-1} mode appears as a broad feature that shifts with λ_{exc} as expected for direct excitation within the "trap" (see Figure 3a). It represents either a phonon mode of the protein or an intermolecular vibration.[20,30]

Fluorescence spectra of the CP47−antenna complex are shown in Figure 2b. On excitation to the blue side of 680 nm, the emission has its maximum at ∼691 nm and no line narrowing is observed for the reasons discussed in relation to the RC. For $\lambda_{exc} > 680$ nm, there is FLN and a low-frequency peak appears at ∼20 cm^{-1} (see also Figure 3b), as for the RC but somewhat broader, which shifts with excitation wavelength. Notice that FLN in CP47 starts at about 4 nm to the red as compared to that in the RC. For $\lambda_{exc} \geq 686$ nm, a broad feature at ∼75 ± 5 cm^{-1} from λ_{exc} becomes visible (see also Figure 3b) that shifts with λ_{exc}.

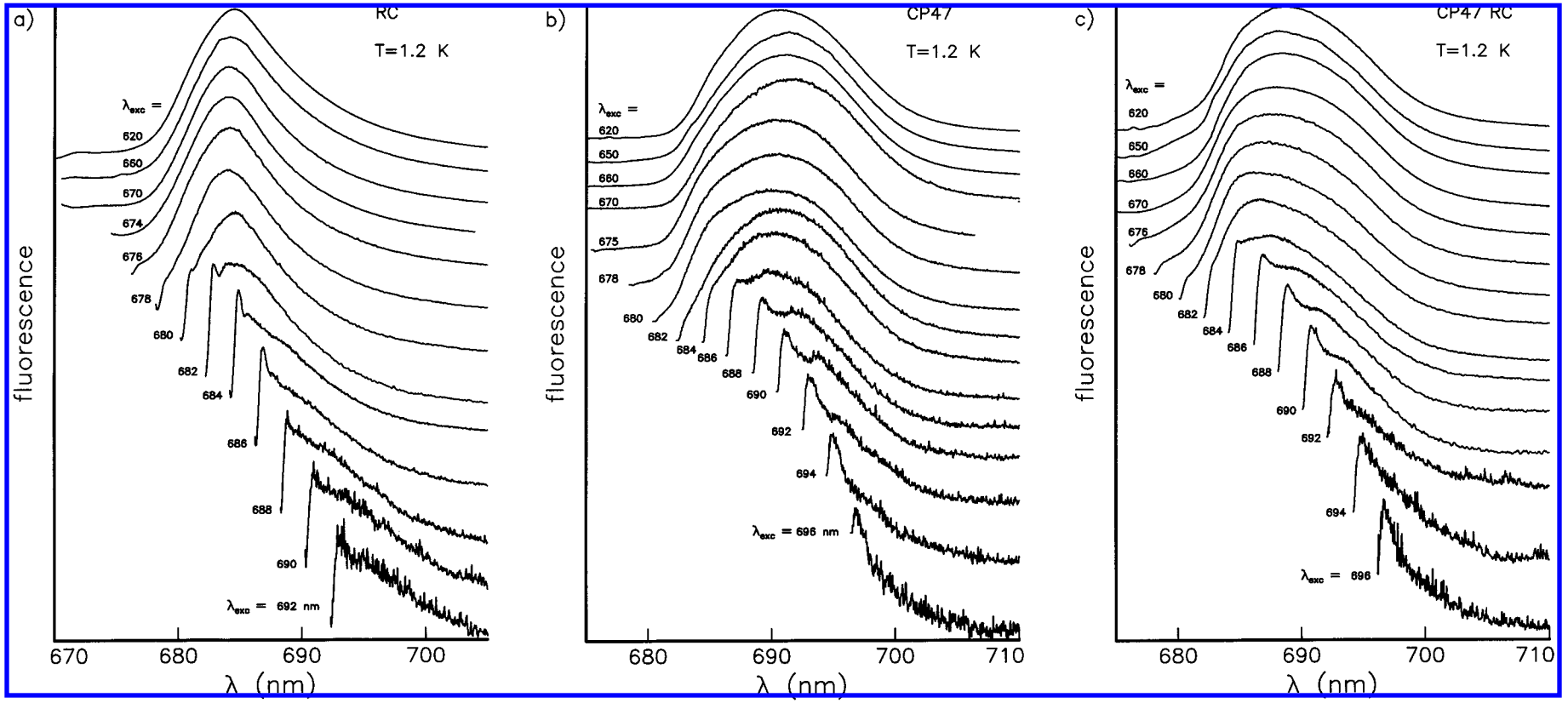

Figure 2. Broad-band and line-narrowing fluorescence spectra at 1.2 K for excitation wavelengths between 620 and ~700 nm. The spectra have been corrected for the sensitivity of the photomultiplier. They are displaced relative to each other. (a) The isolated reaction center of PS II. (b) The CP47 core antenna. (c) The CP47−RC complex.

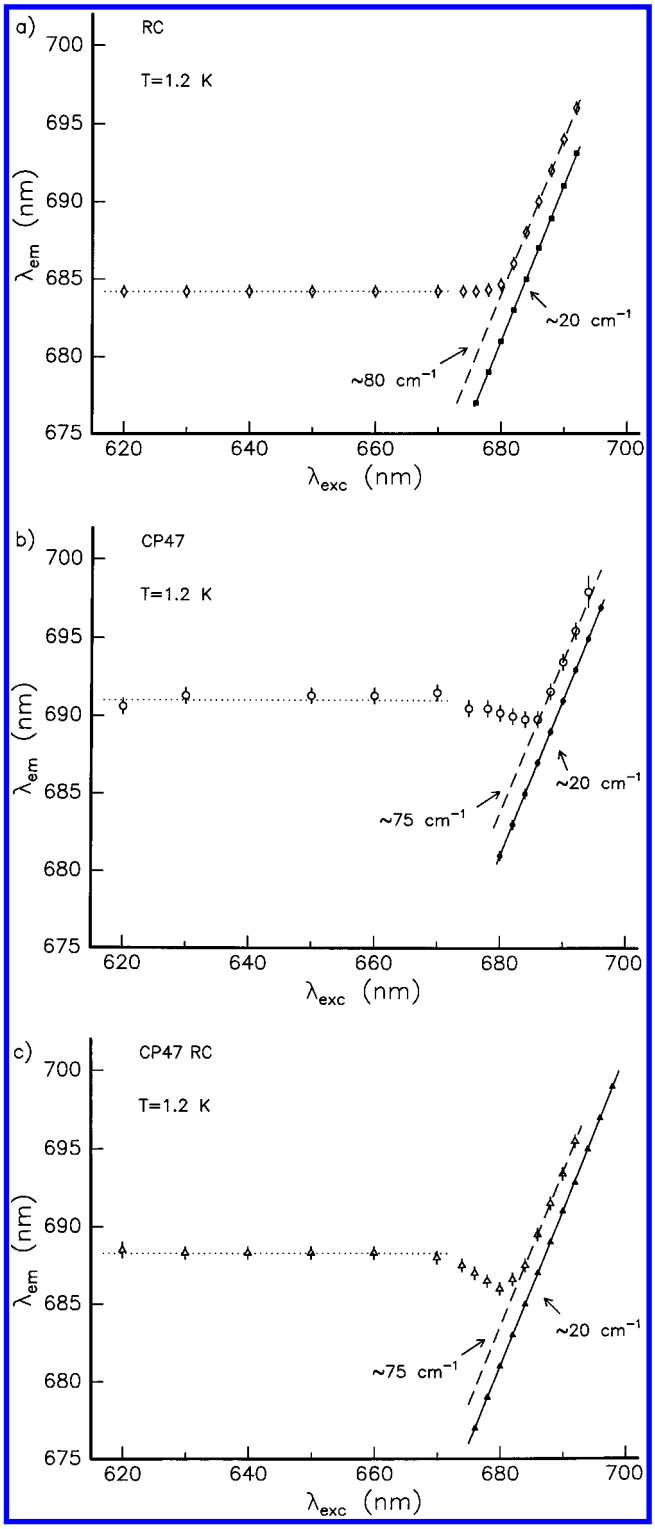

Figure 3. Position of the maxima λ_{em} of the fluorescence spectra at 1.2 K as a function of excitation wavelength λ_{exc}. The data were obtained from averages of spectra such as those shown in Figure 2. The curves traced through the data are guides for the eye. Two types of maxima have been plotted. The closed symbols represent the sharp maximum at about 20 cm^{-1} from the laser excitation wavelength at $\lambda_{exc} \geq 676$ nm for the RC (Figure 3a) and the CP47−RC (Figure 3c) complexes, and $\lambda_{exc} \geq 680$ nm for the CP47−antenna (Figure 3b). The open symbols represent the broad maximum. In the spectral region, where the 20 cm^{-1} mode is observed, the position of the broad maximum approximately reflects a 75−80 cm^{-1} mode. In this region, the data points follow straight lines with a slope $d\lambda_{em}/d\lambda_{exc} = 1$. For an explanation of the "dip", see text.

Figure 2c shows fluorescence spectra of CP47−RC. FLN is observed for $\lambda_{exc} \geq 676$ nm, as for the RC, and the lowest frequency peak is again located at ~20 cm^{-1}, whereas a broad feature is discernible at ~75 ± 5 cm^{-1} from the laser frequency when $\lambda_{exc} \geq 684$ nm (see also Figure 3c). Since the FLN spectra of CP47−RC at $\lambda_{exc} \geq 686$ nm are very similar to those of CP47 at the same excitation wavelengths, we conclude that the red-most "trap" pigments in CP47−RC are the same as those in CP47. This implies that at least part of the excitation energy is transferred "downhill" within the CP47−RC complex to its CP47 component. Note, however, that FLN in CP47−RC starts further to the blue than in CP47, which suggests that the RC component of CP47−RC also acts as a fluorescing "trap". Further evidence for this hypothesis is given in parts a−c of Figures 3.

It is striking that the λ_{em} vs λ_{exc} data for CP47 shown in Figure 3b exhibit a small "dip" around 684 nm of ~1.5 nm, not visible in the RC (Figure 3a). A similar "dip" is observed for CP47−RC (Figure 3c), but it is more pronounced than that in CP47 (2.5 nm versus 1.5 nm) and occurs further to the blue at ~680 nm. We believe that the "dip" in the λ_{em} vs λ_{exc} plots appears for the following reason. Assume that the inhomogeneous distribution of "trap" pigments absorbing furthest to the red have their absorption maximum well separated from the maximum of the pigments undergoing "downhill" energy transfer. If only the latter pigments are excited ($\lambda_{exc} = 620-670$ nm), they will transfer energy "downhill" and the emission will be nonselective and broad from the "traps" with λ_{em} = constant, independent of λ_{exc} (horizontal dotted line in parts a−c of Figure 3). In the overlapping region where "traps" and transferring molecules absorb simultaneously, the emission will shift toward the blue while λ_{exc} shifts to the red because an increasing fraction of the "trap" pigments absorbing in the blue wing of their inhomogeneous distribution contributes selectively to the emission (the region of the "dip" in parts b and c of Figure 3). For example, in Figure 3c at $\lambda_{exc} = 678$ nm, some pigments will transfer energy "downhill" and fluoresce at $\lambda_{em} \approx 688$ nm, whereas the rest of the pigments, the "traps", fluoresce at λ_{em} close to λ_{exc}. The observed fluorescence, thus, appears between 678 and 688 nm. When λ_{exc} is shifted further to the red and "trap" pigments are almost exclusively excited, the emission of the latter takes over. Now λ_{em} will shift to the red together with λ_{exc} (Figure 3, right parts). We think that the "dip" is more pronounced in CP47−RC than in CP47 because CP47−RC has two emitting "traps", one from the RC component absorbing at ~682 nm, which "pulls" the emission toward the blue, and the other from the CP47 component absorbing at ~690 nm (see parts b and c of Figure 3). The RC probably does not show a "dip" (Figure 3a) because the spectral distance between the maximum of the "trap" absorption and the maximum of the absorption of the pigments transferring energy is relatively small. Apparently, there is no "competition" region in which the pigments transferring energy do emit more to the red than the "trap" pigments excited in their blue wing.

Similar λ_{em} vs λ_{exc} curves as those plotted in parts a−c of Figure 3 have been reported for the B800-band of the LH2−antenna complexes of purple bacteria.[37] The "dip" in the B800-band, however, was found to be twice as large as that in CP47−RC. It was explained in ref 37 by a competition of *interband* (between B800 and B850) and *intraband* (within B800) energy-transfer processes. The spectral region over which line-narrowing and nonselective fluorescence are simultaneously present is apparently much wider in the B800-band of LH2 than in the complexes studied here. "Dips" of 1 ± 0.5 nm have also been observed for isolated photosystem I particles.[38]

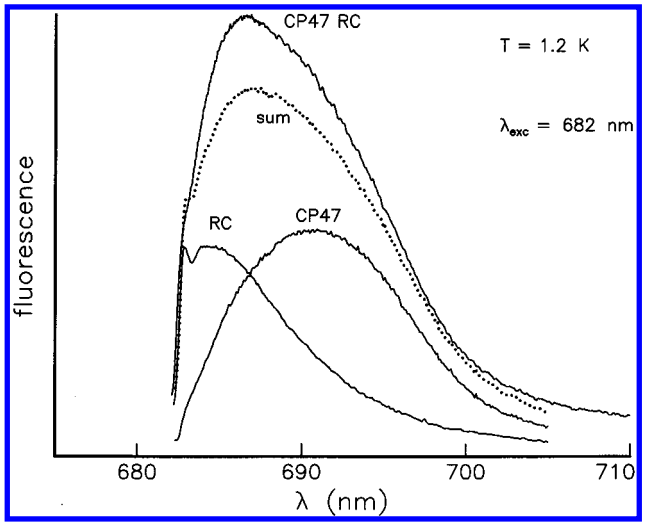

Figure 4. Fluorescence spectra of the three complexes RC, CP47, and CP47−RC at 1.2 K, excited at 682 nm with a power density of $P/A \approx 5$ mW/cm^2. The intensity of the individual RC and CP47 spectra were taken in such a way that their sum (dotted line) yielded a spectrum that, in its intensity and shape, resembles as much as possible the fluorescence spectrum of CP47−RC.

We further see in Figure 3c that the region in which the 20 cm^{-1} peak is observed stretches further to the blue ($\lambda_{exc} \geq 676$ nm) than in CP47, as does the region of the "dip" (670 nm $< \lambda_{exc} <$ 682 nm). We suggest that this blue shift arises because the RC component of CP47−RC, when excited, does not transfer all the excitation energy to the CP47 component, but part of the energy is trapped in the RC distribution at ∼682 nm and emitted as fluorescence at ∼684 nm. In the spectral region of the "dip" (see Figure 3c), the RC "trap" is directly excited and, therefore, the ∼75 cm^{-1} broad phonon band is shifted somewhat more to the blue with respect to that in CP47 (see Figure 2b). This behavior is also illustrated in Figure 4, where the fluorescence spectra of all three complexes excited at 682 nm have been plotted. The intensities of the RC and CP47 spectra were scaled in such a way that the sum of the two spectra (dotted line) resembles as much as possible the measured fluorescence spectrum of CP47−RC. The intensity of the latter, however, could not be completely reproduced (see comments related to Figure 1a).

3.2. Distribution of "Trap" Pigments Determined by Hole Burning. To identify the "trap" pigments absorbing in the red wing of the Q_y-band of the CP47 and CP47−RC complexes, we have performed hole-burning (HB) experiments with megahertz resolution as a function of excitation wavelength λ_{exc} and temperature T between 1.2 and 4.2 K. The spectral distribution of these pigments was determined, as previously for the RC,[21] from the relative depth D (%) of the holes measured as a function of λ_{exc} between 682 and 692 nm, at constant burning fluence density ($Pt_b/A = 0.3$ mJ/cm^2), at 1.2 K. Since the results for CP47 in the red-most wing of the absorption band are very similar to those found for CP47−RC, we only show the results for the latter.

In Figure 5a, D (%) versus λ_{exc} is plotted together with the red wing of the fluorescence excitation spectrum (dashed line). Relatively narrow holes (∼0.6 GHz) were burnt, which change their depth but not their width as a function of λ_{exc}. This HB method selects pigments that are involved in a dynamic process characterized by a specific decay time.[21,37,39] The curve traced through the data is a guide for the eye. Multiplying this curve by the profile of the fluorescence excitation spectrum yields an approximate Gaussian profile (see Figure 5b), with a maximum

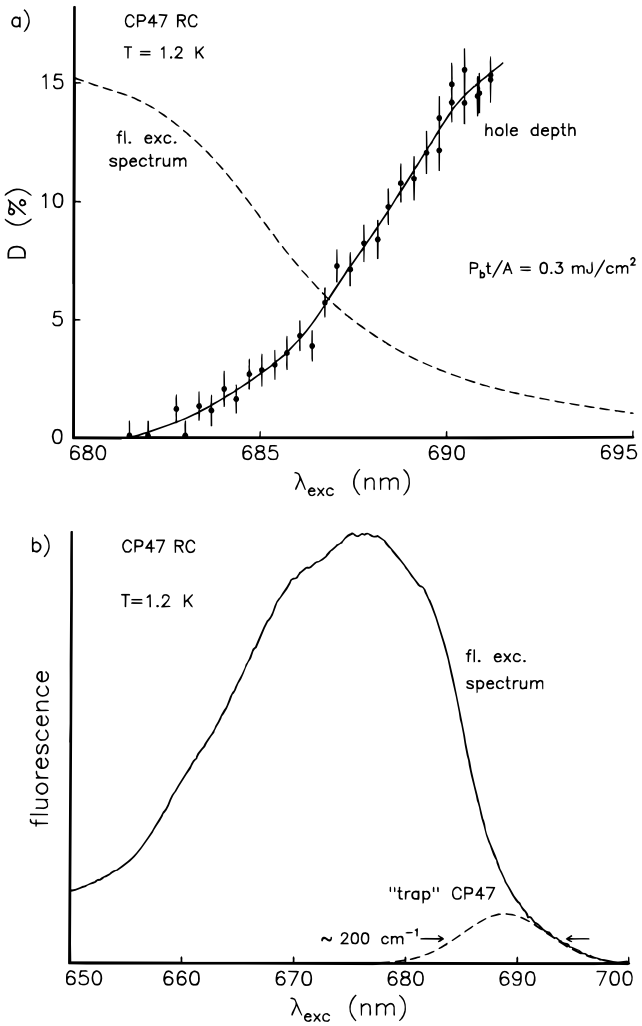

Figure 5. (a) Relative hole depth D (%) as a function of excitation wavelength λ_{exc} (solid line) together with the profile of the red wing of the fluorescence excitation spectrum of CP47−RC at 1.2 K (dashed line). The holes were burnt with a fluence density $Pt_b/A = 0.3$ mJ/cm^2. Notice that for this burning fluence no holes are detected at $\lambda_b \approx 682$ nm (the maximum of the absorption of the RC "trap"). (b) Spectral distribution of the red-most absorbing "trap" pigments in CP47−RC (dashed line) within the fluorescence excitation spectrum (solid line).

at 688.9 ± 0.4 nm and a width (fwhm) = 200 ± 15 cm^{-1}. The height of the "trap" distribution has been normalized to fit the wing of the fluorescence excitation spectrum of CP47−RC. We attribute this "trap" to pigments belonging to the CP47 component of CP47−RC. The argument is based on the following facts: (i) the RC does not absorb at wavelengths longer than 690 nm (see Figure 1a) and (ii) no holes could be burnt at 682 nm (the maximum of the "trap" distribution of RC) with the rather low burning fluence densities used here. For comparison, the maximum of the RC "trap" at ∼682 nm[21] in the RC is about 7 nm to the blue of the "trap" of the CP47, its inhomogeneous width is somewhat smaller (∼145 cm^{-1}), and the relative intensity is much larger than that of CP47. The difference in relative intensity can be understood if we assume that each "trap" distribution would contain the oscillator strength of one pigment and the RC consists of eight chlorophyll-like molecules, whereas CP47−RC is built up by ∼22 chlorophylls.

To determine the "effective" homogeneous line width Γ'_{hom} of the "traps" of CP47−RC, we have measured the hole width at a given temperature as a function of burning fluence density and extrapolated it to $Pt_b/A \rightarrow 0$. The results are shown in parts

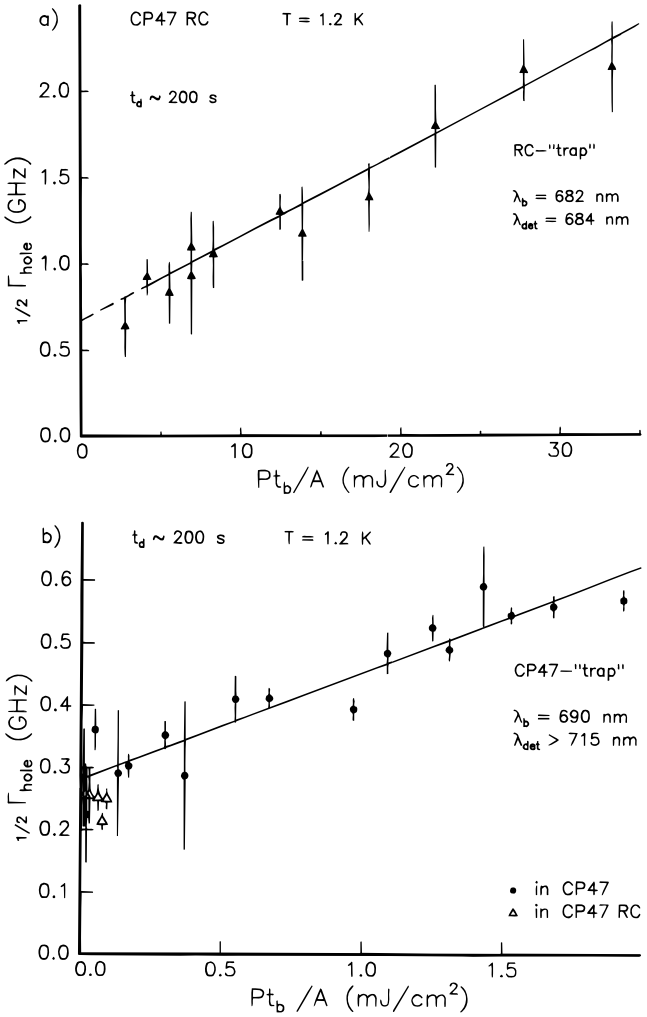

Figure 6. (a) Half the holewidth $^1/_2\Gamma_{hole}$ as a function of burning fluence density Pt_b/A for CP47−RC at 1.2 K. The holes were burnt at λ_b = 682 nm and detected at λ_{det} = 684 nm (closed triangles). A linear extrapolation of $^1/_2\Gamma_{hole}$ to $Pt_b/A \rightarrow 0$ yields a value that is significantly larger than the "effective" homogeneous line width (see text). (b) $^1/_2\Gamma_{hole}$ versus Pt_b/A at λ_b = 690 nm in CP47, and detected at λ_{det} > 715 nm (black dots). The data extrapolated to $Pt_b/A \rightarrow 0$ represent the values of Γ'_{hom}. The widths of holes burnt at 690 nm in CP47−RC (open triangles) extrapolate to the same value as those burnt at the same wavelength in CP47.

a and b of Figure 6 for CP47−RC at 1.2 K burnt at two different wavelengths, λ_b = 682 nm (the maximum of the absorption of the RC "traps"), with λ_{det} = 684 nm (the maximum of the fluorescence of the RC) (Figure 6a), and λ_b = 690 nm (the maximum of the absorption of the CP47 "traps"), with λ_{det} > 715 nm (Figure 6b, open triangles). Since the RC does not absorb at 690 nm (see Figure 1a), only pigments belonging to the CP47 component of CP47−RC are excited when burning a hole at this wavelength. These holes are a few hundred megahertz broad and could be observed for burning fluence densities down to 50 μJ/cm^2 (see Figure 6b). The hole widths plotted with black dots in Figure 6b have been measured in the "trap" of the CP47 sample. They extrapolate to $^1/_2\Gamma_{hole} = \Gamma'_{hom}$ = 220 MHz for $Pt_b/A \rightarrow 0$. The open triangles for the CP47 "trap" of CP47−RC extrapolate to the same value.

When burning in CP47−RC at λ_b = 682 nm, pigments belonging to the RC and to CP47 are simultaneously excited (see Figure 1a). If we detect at λ_{det} = 684 nm, the observed fluorescence is predominantly emitted by pigments belonging to the RC (see Figure 4). The hole width, thus, mainly

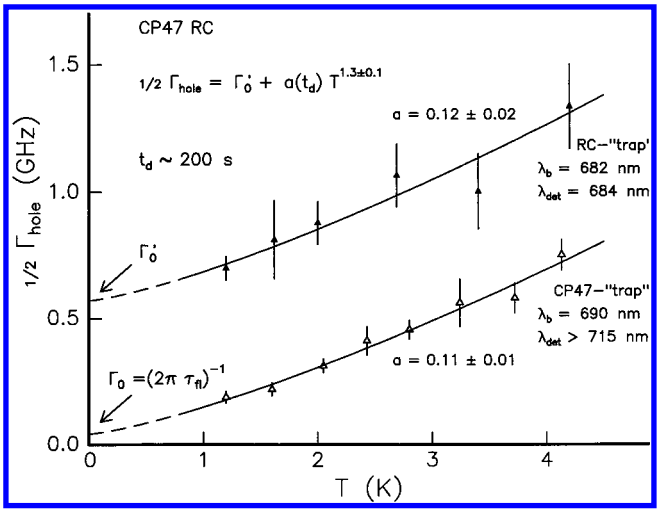

Figure 7. Temperature dependence of $^1/_2\Gamma_{hole}$ between 1.2 and 4.2 K for the RC "trap" in CP47−RC, at λ_b = 682 nm and λ_{det} = 684 nm (closed triangles), and the CP47 "trap" in CP47−RC at λ_b = 690 nm and λ_{det} > 715 nm (open triangles), at delay time $t_d \approx$ 200 s. $^1/_2\Gamma_{hole}$ follows a $T^{1.3\pm0.1}$ power law and displays the same coupling constant a = 0.12 ± 0.02 GHz/K$^{1.3}$ for both excitation wavelengths. For λ_b = 690 nm, $^1/_2\Gamma_{hole}$ extrapolates to $\Gamma_0 = (2\pi\tau_{fl})^{-1}$ = 40 ± 10 MHz for $T \rightarrow 0$, with τ_{fl} = 4 ± 1 ns being the fluorescence lifetime. These pigments belong to the CP47 "trap" within CP47−RC. For λ_b = 682 nm, $^1/_2\Gamma_{hole}$ extrapolates to a value $\Gamma'_o \gg \Gamma_0$. In this spectral region, there are RC "traps" and pigments that transfer energy "downhill" within CP47−RC (see text).

corresponds to "trap" pigments of the RC component of CP47−RC. The data in Figure 6a, measured down to $Pt_b/A \approx$ 3 mJ/cm^2, extrapolate to $^1/_2\Gamma_{hole} \approx$ 700 MHz for $Pt_b/A \rightarrow 0$. This value, however, is much larger than that of the "trap" pigments in the RC, which was found to be ~260 MHz at 1.2 K.[21] We attribute this difference to power-broadening effects, because in the present experiments 5 times larger burning fluence densities were needed as compared to those in ref 21. The reason for this is that the holes had to be detected through a monochromator that reduced the signal-to-noise ratio and we could not use Pt_b/A values lower than ~3 mJ/cm^2. The observed hole widths may also contain a minor contribution from "downhill" energy transfer from CP47 pigments excited at 682 nm in CP47−RC to CP47 pigments absorbing further to the red that emit at 684 nm. Since the holes are detected in fluorescence excitation, any contribution from P680 is not observed.[21]

The temperature dependence Γ'_{hom} of the CP47 "traps" in CP47−RC, absorbing at λ_b = 690 nm and detected at λ_{det} > 715 nm (open triangles), is shown in Figure 7. The data follow a $T^{1.3}$ power law.

$$\Gamma'_{hom} = \Gamma_0 + a(t_d)T^{1.3\pm0.1} \qquad (2)$$

characteristic for dephasing in doped organic glasses.[28,29,40,41] Such a power law has also been found by us for the isolated RC[21] and for subunits of the LH1−antenna complex of purple bacteria.[42] Although the T dependence of Γ'_{hom} is that found in glasses, the dependence on delay time between burning and probing the hole is different.[22,39] The lower curve of Figure 7 extrapolates to the fluorescence lifetime-limited value $\Gamma_0 = (2\pi\tau_{fl})^{-1}$ for $T \rightarrow 0$, with τ_{fl} = 4 ± 1 ns. The results demonstrate that the red-most absorbing pigments of CP47−RC within the Q_y band undergo dephasing and decay but do not transfer energy "downhill"; they act as "traps" for the excitation energy. The same result was found for the "traps" in isolated CP47 burnt at λ_b = 690 nm.[22]

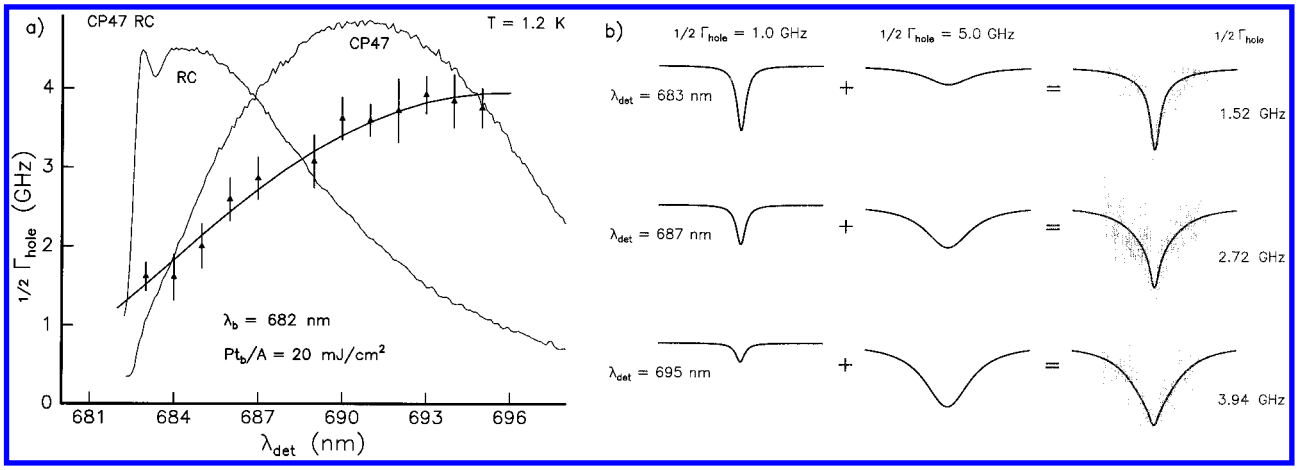

Figure 8. (a) $^1/_2\Gamma_{hole}$ versus λ_{det} for holes burnt at $\lambda_b = 682$ nm in CP47−RC at 1.2 K. A large burning fluence density (20 mJ/cm^2; see Figure 6b) was used in order to be able to detect a hole through the monochromator at every λ_{det}. The thin lines represent the fluorescence spectra of the isolated RC and CP47 excited at 682 nm. The thick line was obtained from a model in which the hole-burning data were simulated (see Figure 8b). (b) Model to explain the data of figure 8a. Two holes assumed to be burnt at 682 nm with widths $^1/_2\Gamma_{hole} = 1.0$ and 5.0 GHz and varying depths. They were added to yield a hole at each λ_{det}. The narrow hole is supposed to be burnt in the "trap" of the RC component of CP47−RC, whereas the broad hole is associated with CP47 pigments that transfer energy "downhill". The relative depths of the two holes at a given λ_{det} were taken as explained in the text. The non-Lorentzian holes resulting from the sum of the two holes fit the measured holes (gray line) well.

As mentioned in the Introduction, a dephasing time of ∼50 ps was reported for the 690 nm state in CP47,[16] a value much shorter than the 4 ns lifetime obtained here. We think that this discrepancy originates from the fact that the holes of ref 16 were detected in absorption with a 10^6 times higher burning fluence density than used by us in fluorescence excitation. The latter method is usually more sensitive than the former. Furthermore, the hole widths in ref 16 were determined at 4.2 K and neither extrapolated to $Pt_b/A \rightarrow 0$ nor to $T \rightarrow 0$.

The upper curve in Figure 7 represents the temperature dependence of the extrapolation value of $^1/_2\Gamma_{hole}$ for $Pt_b/A \rightarrow 0$ of the RC "trap" in CP47−RC, burnt at $\lambda_b = 682$ nm and detected at $\lambda_{det} = 684$ nm (closed triangles). Although the curve follows a $T^{1.3}$ power law, it extrapolates to $\Gamma'_0 \approx 600$ MHz for $T \rightarrow 0$, a value much larger than the fluorescence lifetime-limited value of $\Gamma_0 \approx 40$ MHz measured at $\lambda_b = 690$ nm (see lower curve). As already mentioned, Γ'_0 is most probably power-broadened and may contain a contribution of "downhill" energy transfer from CP47 pigments absorbing at 682 nm to CP47 pigments lying further to the red. The coupling constant $a(t_d) = 0.12 \pm 0.02$ GHz/K$^{1.3}$ of the upper curve is equal, within the error bar, to that of the lower curve, which suggests that CP47−RC as a whole is responsible for the dephasing, and not the individual "trap" pigments of the RC and CP47 components.

In Figure 8a, the width $^1/_2\Gamma_{hole}$ of a hole burnt in CP47−RC at $\lambda_b = 682$ nm is plotted as a function of detection wavelength. We see that the value of $^1/_2\Gamma_{hole}$ gradually increases from ∼1.5 GHz at $\lambda_{det} = 683$ nm to ∼3.7 GHz at $\lambda_{det} = 695$ nm. This behavior can be explained by assuming that the observed hole is the sum of two holes, one burnt in the "trap" pigments of the RC and the other burnt in CP47 pigments, both absorbing at 682 nm, as illustrated in Figure 8b. If we assume that the hole in the "trap" of the RC is power-broadened and has a width $^1/_2\Gamma_{hole} = 1.0$ GHz and the hole in the CP47 pigments is broader due to "downhill" energy transfer from 682 nm to the "trap" of CP47, $^1/_2\Gamma_{hole} = 5.0$ GHz, we can fit the data of Figure 8a very well. The ratio in which we have summed the two holes depends on the detection wavelength. For example, at $\lambda_{det} = 683$ nm, the observed fluorescence mainly originates from the "trap" pigments of the RC because there is almost no fluorescence from the CP47 pigments at this detection wavelength (see Figure 8a, thin lines) and the holes are relatively narrow. At an intermediate detection wavelength, say $\lambda_{det} = 687$ nm, the measured hole will be the sum of two Lorentzians with relative depths determined by the fluorescence intensity contributions of the RC and the CP47 "traps" at this wavelength. This ratio, which can be estimated from the individual fluorescence spectra of the RC and CP47 at each wavelength, is equal to 1 at 687 nm. At $\lambda_{det} = 695$ nm, the fluorescence signal arises mainly from the "trap" of CP47 and the holes are broad. We conclude from Figure 8b that the resulting non-Lorentzian holes simulate well the experimentally obtained holes. The curve traced in Figure 8a, which was obtained by summing up the two Lorentzian holes as shown in Figure 8b, fits the data well and supports our interpretation. The value $^1/_2\Gamma_{hole} = 5.0$ GHz yields a lower limit for the energy-transfer time $\tau_{ET} \geq (2\pi^1/_2\Gamma_{hole})^{-1} \approx 30$ ps, which is significantly longer (and, therefore, the hole width much smaller) than that of ref 16, where a "downhill" transfer time of ∼10 ps was attributed to pigments absorbing around 684 nm.

4. Conclusions

We have demonstrated that, because of their wavelength selectivity, hole-burning (HB) and FLN experiments can be combined in a useful way to unravel spectral distributions of "trap" pigments in large photosynthetic complexes such as CP47−RC, CP47, and the RC of PS II at liquid-He temperatures.

The fluorescence spectra of these complexes show line narrowing only in the region of excitation wavelengths λ_{exc} corresponding to the absorption of their "trap" pigments. For λ_{exc} to the blue side of this region, broad fluorescence spectra are observed that reflect the presence of nonselective "downhill" energy transfer. For the RC (Figures 2a and 3a), the bands are broad with a maximum at $\lambda_{em} \approx 684$ nm if $\lambda_{exc} < 676$ nm. FLN has its onset at $\lambda_{exc} \geq 676$ nm. In this region, a sharp peak at ∼20 cm^{-1} and a broad one at ∼80 ± 5 cm^{-1} appear, which shift to the red with λ_{exc} in such a way that $d\lambda_{em}/d\lambda_{exc} = 1$. The results imply that $\Gamma'_{hom} \ll \Gamma_{inh}$, which was indeed verified by HB.[21] The peaks at ∼20 and 80 cm^{-1} represent low-frequency modes, either phonon modes of the protein[33] and/or intermolecular vibrational modes.[20,30] We have found similar FLN results for CP47 (Figures 2b and 3b), but the onset of this

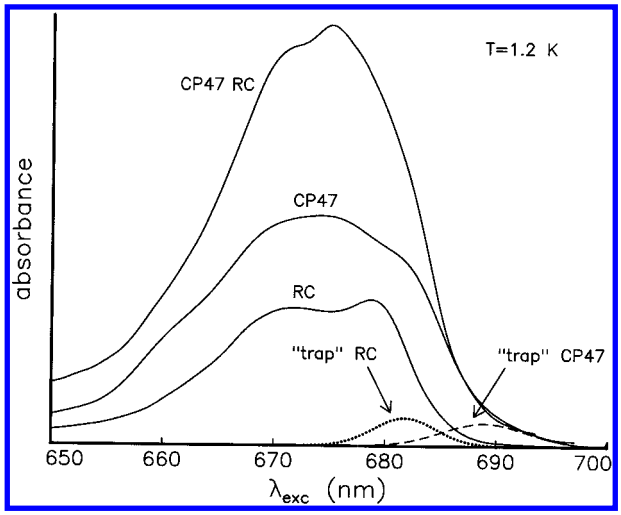

Figure 9. Summary of the "trap" distributions in the RC, CP47, and CP47−RC complexes. The three absorption spectra are the same as in Figure 1. The "trap" distribution of the CP47 antenna (dashed line), which is also present in the CP47−RC complex, has been normalized to fit the red wing of the CP47 and CP47−RC absorption spectra. The distribution of "trap" pigments of the RC (dotted line) has been normalized to the RC absorption spectrum as described in ref 17. RC "traps" are also present in the CP47−RC complex, as shown in this work.

region ($\lambda_{exc} \geq 780$ nm) is shifted ~4 nm to the red as compared to the RC. The low-frequency modes are also similar, a sharp peak appears at ~20 cm^{-1} and a broad one at 75 ± 5 cm^{-1}. The dependence of λ_{em} on λ_{exc}, however, shows a "dip" not observed in the RC. It is located in a spectral region of "competition" between pigments transferring energy "downhill" and "trap" pigments that absorb at the same λ_{exc}. This "dip" is even more pronounced and blue-shifted in CP47−RC (Figures 2c and 3c), probably due to the presence of two "traps". In contrast to CP47, CP47−RC shows FLN for $\lambda_{exc} \geq 676$ nm, as does the RC. The shapes of the FLN spectra for $\lambda_{exc} \geq 688$ nm in CP47−RC, however, are almost identical to those of CP47. These results, together with the shape and position of the "dip", strongly suggest that there are two "traps" in CP47−RC, one corresponding to the CP47 component and the other to the RC component of the complex.

From the hole depth as a function of excitation wavelength, we have obtained the spectral distribution of the red-most "trap" pigments in the RC,[21] CP47, and CP47−RC (Figure 5). We conclude that in CP47−RC these "traps" absorbing at ~690 nm belong to the CP47 component of the complex. The "effective" homogeneous line width of these pigments, which was measured as a function of temperature, extrapolates to the fluorescence lifetime-limited value $\Gamma_0 = (2\pi\tau_{fl})^{-1}$ for $T \rightarrow 0$, with $\tau_{fl} = 4 \pm 1$ ns, proving that they are indeed "traps" for the excitation energy (Figure 6b).

The increase of the width of the holes burnt at 682 nm in CP47−RC with detection wavelength λ_{det} from 683 to 695 nm (Figure 7) can be explained by assuming that the measured hole is the sum of two holes, a relatively narrow one burnt in the "trap" pigments of the RC component at 682 nm and a somewhat broader one burnt in CP47 pigments, with the latter absorbing at the same wavelength but transferring energy "downhill". If we take the relative depths of the two holes at a given λ_{det} equal to the relative intensities of the corresponding fluorescence spectra of the RC and CP47 at the same wavelength, the data can be simulated well.

We have summarized our results in Figure 9, where the spectral distributions of the RC and CP47 "trap" pigments within the RC, CP47, and CP47−RC complexes are plotted, together with the corresponding absorption spectra. CP47−RC has two types of "traps", the RC one with a maximum at ~682 nm and the CP47 one with a maximum at ~690 nm, each fluorescing independently when excited. These "traps" probably consist of pigments with an oscillator strength corresponding to that of one pigment. This argument is based on the small ratio of the areas of each "trap" distribution to that of the absorption spectrum of its corresponding complex. We conclude that the two "traps" in CP47−RC, which have partly overlapping spectra, have to be either at a distance from each other that is significantly larger than the Förster radius $R_0 \approx 3-8$ nm or they have to have unfavorable relative orientations such that energy transfer cannot take place from the RC to the CP47 "trap" at low temperature.

Acknowledgment. We thank H. van Roon for preparing the samples and F. Vacha for valuable discussions. J. H. van der Waals is acknowledged for his constructive comments. The investigations were financially supported by The Netherlands Foundation for Physical Research (FOM) and the Council for Chemical Research of The Netherlands Organization for Scientific Research (CW-NWO).

References and Notes

(1) Diner, B. A.; Babcock, G. T. In *Oxygenic Photosynthesis: The Light Reactions*; Ort D. R., Yocum, C. F., Eds.; Kluwer: Dordrecht, 1996; p 213−247.
(2) Hankamer, B.; Barber, J.; Boekema, E. J. *Annu. Rev. Plant Physiol. Plant Mol. Biol.* **1997**, *48*, 641−671 and references therein.
(3) van Grondelle, R.; Dekker, J. P.; Gillbro, T.; Sundström, V. *Biochim. Biophys. Acta* **1994**, *1187*, 1−65 and references therein.
(4) Boekema, E. J.; van Roon, H.; Dekker, J. P. *FEBS Lett.* **1998**, *424*, 95 and references therein. Eijckelhoff, C.; Dekker, J. P.; Boekema E. J. *Biochim. Biophys. Acta* **1997**, *1321*, 10.
(5) Nanba, O.; Satoh, K. *Proc. Natl. Acad. Sci. U.S.A.* **1987**, *84*, 109.
(6) Dekker, J. P.; Hassoldt, A.; Petterson, Å.; van Roon, H.; Groot, M. L.; van Grondelle, R. In *Photosynthesis: from Light to Biosphere*; Mathis, P., Ed.; Kluwer: Dordrecht, 1995; Vol. I, p 53.
(7) Rhee, K. H.; Morris, E. P.; Zheleva, D.; Hankamer, B.; Kühlbrandt, W.; Barber, J. *Nature* **1997**, *389*, 522.
(8) Michel, H.; Deisenhofer, J. *Biochemistry* **1988**, *27*, 1.
(9) Nugent, J. H. A. *Eur. J. Biochem.* **1996**, *237*, 519.
(10) Svensson, B.; Etchebest, C.; Tuffery, P.; van Kan, P. J. M.; Smith, J.; Styring, S. *Biochemistry* **1996**, *35*, 14486.
(11) Greenfield, S. R.; Wasielewski, M. R. *Photosynth. Res.* **1996**, *48*, 83 and references therein.
(12) Klug, D. R.; Durrant, J. R.; Barber, J. *Philos. Trans. R. Soc. London, Ser. A* **1998**, *356*, 449 and references therein.
(13) Groot, M. L.; van Mourik, F.; Eijckelhoff, C.; van Stokkum, I. H. M.; Dekker, J. P.; van Grondelle, R. *Proc. Natl. Acad. Sci. U.S.A.* **1997**, *94*, 4389.
(14) Bricker, T. M. *Photosynth. Res.* **1990**, *24*, 1.
(15) Kwa, S. L. S.; van Kan, P. J. M.; Groot, M. L.; van Grondelle, R.; Yocum, C. F.; Dekker, J. P. In *Research in Photosynthesis*; Murata, N., Ed.; Kluwer: Dordrecht, 1992; Vol. I, p 263.
(16) Chang, H.-C.; Jankowiak, R.; Yocum, C. F.; Picorel, R.; Alfonso, M.; Seibert, M.; Small, G. J. *J. Phys. Chem.* **1994**, *98*, 7717.
(17) Groot, M. L.; Peterman, E. J. G.; van Stokkum, I. H. M.; Dekker, J. P.; van Grondelle, R. *Biophys J.* **1995**, *68*, 281.
(18) van Dorssen, R. J.; Plijter, J. J.; Dekker, J. P.; den Ouden, A.; Amesz, J.; van Gorkom, H. J. *Biochim. Biophys. Acta* **1987**, *890*, 134.
(19) Chang, H.-C.; Jankowiak, R.; Reddy, N. R. S.; Yocum, C. F.; Picorel, R.; Seibert, M.; Small, G. J. *J. Phys. Chem.* **1994**, *98*, 7725.
(20) Peterman, E. J. G.; van Amerongen, H.; van Grondelle, R.; Dekker, J. P. *Proc. Natl. Acad. Sci. U.S.A.* **1998**, *95*, 6128.
(21) Groot, M. L.; Dekker, J. P.; van Grondelle, R.; den Hartog, F. T. H.; Völker, S. *J. Phys. Chem.* **1996**, *100*, 11488.
(22) den Hartog, F. T. H.; van Papendrecht, C.; Störkel, U.; Völker, S. *J. Phys. Chem.*, submitted.
(23) Dekker, J. P.; Bowly, N. R.; Yocum, C. F. *FEBS Lett.* **1989**, *254*, 150.
(24) Dekker, J. P.; Betts, S. D.; Yocum, C. F.; Boekema, E. J. *Biochemistry* **1990**, *29*, 3220.
(25) Eijckelhoff, C.; Dekker, J. P. *Biochim. Biophys. Acta* **1995**, *1231*, 21.

(26) Kwa, S. L. S.; Newell, W. R.; van Grondelle, R.; Dekker, J. P. *Biochim. Biophys. Acta* **1992**, *1099*, 193.

(27) van Kan, P. J. M.; Groot, M. L.; van Stokkum, I. H. M.; Kwa, S. L. S.; van Grondelle, R.; Dekker, J. P. In *Research in Photosynthesis*; Murata, N., Ed.; Kluwer: Dordrecht 1992; Vol. I, p 271. van Kan, P. J. M.; Groot, M. L.; Kwa, S. L. S.; Dekker, J. P.; van Grondelle, R. In *The Photosynthetic Bacterial Reaction Center*; Breton, J., Verméglio, A., Eds.; Plenum Press: New York, 1992; Vol. II, p 411.

(28) Koedijk, J. M. A.; Wannemacher, R.; Silbey, R. J.; Völker, S. *J. Phys. Chem*. **1996**, *100*, 19945.

(29) Creemers, T. M. H.; Koedijk, J. M. A.; Chan, I. Y.; Silbey, R. J.; Völker, S. *J. Chem. Phys.* **1997**, *107*, 4797.

(30) Kwa, S. L. S.; Eijckelhoff, C.; van Grondelle, R.; Dekker, J. P. *J. Phys. Chem*. **1994**, *98*, 7702.

(31) Kwa, S. L. S.; Tilly, N. T.; Eijckelhoff, C.; van Grondelle, R.; Dekker, J. P. *J. Phys. Chem.* **1994**, *98*, 7712.

(32) Groot, M. L.; Peterman, E. J. G.; van Kan, P. J. M.; van Stokkum, I. H. M.; Dekker, J. P.; van Grondelle, R. *Biophys. J.* **1994**, *67*, 318.

(33) Jankowiak, R.; Hayes, J. M.; Small, G. J. *Chem. Rev.* **1993**, *93*, 1471.

(34) van der Laan, H.; Smorenburg, H. E.; Schmidt, Th.; Völker, S. *J. Opt. Soc. Am. B* **1992**, *9*, 931.

(35) Narasimhan, L. R.; Littau, K. A.; Pack, D. W.; Bai, Y. S.; Elschner, A.; Fayer, M. D. *Chem. Rev.* **1990**, *90*, 439 and references therein.

(36) Tang, D.; Jankowiak, R.; Seibert, M.; Yocum, C. F.; Small, G. J. *J. Phys. Chem.* **1990**, *94*, 6519.

(37) De Caro, C.; Visschers, R. W.; van Grondelle, R.; Völker, S. *J. Phys. Chem*. **1994**, *98*, 10584.

(38) Gobets, B.; van Amerongen, H.; Monshouwer, R.; Kruip, J.; Rögner, M.; van Grondelle, R.; Dekker, J. P. *Biochim. Biophys. Acta* **1994**, *1188*, 75.

(39) den Hartog, F. T. H.; Vacha, F.; Lock, A.; Barber, J.; Dekker, J. P.; Völker, S. *J. Phys. Chem. B* **1998**, *102*, 9174.

(40) Völker, S. In *Relaxation Processes in Molecular Excited States*; Fünfschilling, J., Ed.; Kluwer: Dordrecht; p 1989, 113−242 and references therein; *Annu. Rev. Phys. Chem*. **1989**, *40*, 499, and references therein.

(41) Wannemacher, R., Koedijk, J. M. A.; Völker, S. *Chem. Phys Lett*. **1993**, *206*, 1.

(42) Creemers, T. M. H., et al. To be published.